Secure Systems Design and Technology Development. Veliko Tarnovo, Bulgaria
Proceedings of the International Scientific Conference, 2026. Volume II, 457-464

Comparative Analysis of Numerical and Experimental Results in Laser Hardening of 42CrMo4 Steel

Lyubomir Lazov
Rezekne Academy of Riga Technical University
Rezekne, Latvia
lyubomir.lazov@rtu.lv

Nikolay Angelov
Rezekne Academy of Riga Technical University
Rezekne, Latvia
angelov_np@abv.bg

Prodan Prodanov
Center of competence "Smart mechatronic, eco-and energy-saving systems and technologies"
Technical University of Gabrovo
Gabrovo, Bulgaria
pprodanov@tugab.bg

Normunds Teirumnieks
Rezekne Academy of Riga Technical University
Rezekne, Latvia
normunds.teirumnieks@gmail.com

***Abstract*— Laser hardening of steels is a modern technological process widely used in the automotive, aerospace, and tooling industries. In the present study, a comparative analysis between numerical modeling results and experimental data for the laser hardening process of 42CrMo4 steel samples is performed. Numerical calculations were used to determine preliminary operating intervals of power density at different processing speeds, based on the heat conduction equation and the thermal balance equation with applied approximations. For comparison purposes, in-house experimental results obtained using a 4 kW diode laser were employed. A good correlation between the numerical and experimental results is observed. The obtained findings are useful for operators of laser processing systems as well as for researchers in the field of laser hardening of steels.**

Keywords*— *laser hardening, numerical calculations, experiments, power density, speed, operating intervals.

I. INTRODUCTION

In recent decades, laser surface treatment technologies have gained significant importance in modern manufacturing due to their precision, flexibility, and efficiency. Among these technologies, laser hardening has emerged as a highly effective method for improving the surface properties of metallic materials, particularly steels used in demanding engineering applications. The process enables localized heating of the material surface above the austenitization temperature, followed by rapid self-quenching, which leads to the formation of a hardened martensitic layer without affecting the bulk properties of the component [1 – 6].

Laser hardening is widely applied in industries such as automotive, aerospace, and tooling, where components are subjected to severe wear, fatigue, and contact stresses. Compared to conventional heat treatment methods, laser hardening offers several advantages, including minimal distortion, precise control of the treated area, reduced processing time, and the elimination of additional quenching media. These benefits make it particularly suitable for complex geometries and high-value components where dimensional accuracy and surface integrity are critical [7] – [9].

The effectiveness of the laser hardening process depends strongly on the proper selection and control of process parameters, such as laser power, scanning speed, beam size, and interaction time. These parameters directly influence the thermal cycle experienced by the material, which in turn determines the depth of hardening, microstructural transformations, and resulting mechanical properties. However, the optimization of these parameters is a complex task due to the highly transient and nonlinear

Online ISSN 3044-7771
https://doi.org/10.68302/std2026.vol2.208

nature of heat transfer during laser-material interaction [10] – [17].

To address these challenges, numerical modeling has become an essential tool for predicting temperature fields, phase transformations, and hardened layer characteristics. Models based on the heat conduction equation and thermal balance principles allow researchers and engineers to simulate the process under various conditions, reducing the need for extensive experimental trials. Nevertheless, numerical models often rely on simplifying assumptions, such as constant material properties or idealized boundary conditions, which may limit their accuracy in real-world applications [18] – [22].

Therefore, experimental validation remains a crucial step in verifying the reliability of numerical predictions. A comparative approach, combining simulation and experimental investigation, provides deeper insight into the process mechanisms and helps refine modeling strategies. This synergy between numerical and experimental methods enables more accurate determination of optimal processing windows and enhances process stability and repeatability.

The steel grade 42CrMo4 is widely used in engineering applications due to its excellent combination of strength, toughness, and wear resistance. Understanding the response of this material to laser processing conditions is therefore of both scientific and industrial interest.

In the present study, a comparative analysis between numerical modeling results and experimental data for the laser hardening of 42CrMo4 steel is performed. Numerical calculations are used to estimate suitable operating ranges of power density at different processing speeds, based on simplified thermal models. These results are then compared with experimental data obtained from laser hardening tests conducted using a high-power diode laser system. The objective is to evaluate the degree of agreement between predicted and measured outcomes and to assess the applicability of the numerical approach for practical process optimization.

The findings of this work contribute to a better understanding of the relationship between process parameters and hardening results, and they provide useful guidelines for both industrial practitioners and researchers working in the field of laser surface treatment of steels.

II. Materials and Methods

A. Material

42CrMo4 steel is a high-quality steel widely used in industry. It is used in the Automotive Industry for the manufacture of Crankshafts, Connecting rods, Axles and drive shafts Gears and transmission parts. It is used to make High-strength shafts, Bolts and studs, Hydraulic components and Machine tool parts for Mechanical and Heavy Engineering, In the Energy Sector it is used to make Wind turbine components, Power plant shafts and Drilling equipment. It is also used in the Tool and Die Industry.

Table 1 presents the chemical composition of 42CrMo4 steel in accordance with the requirements of the EN 10083. This composition is carefully balanced to ensure an optimal combination of high strength, good hardenability, and fatigue resistance.

Carbon (C), with a content of 0.38–0.45%, determines the potential for achieving high hardness and strength after heat treatment. Chromium (Cr), in the range of 0.90–1.20%, plays a significant role in increasing the hardenability of the steel as well as its wear resistance. In addition, it improves the material's resistance to oxidation and corrosion under moderate conditions. The addition of molybdenum (Mo) (0.15–0.30%) contributes to increased strength at elevated temperatures and helps reduce temper embrittlement. Molybdenum also improves creep resistance under load. Manganese (Mn) (0.60–0.90%) enhances hardenability and helps bind sulfur through the formation of manganese sulfides, thereby reducing the detrimental effect of sulfur on mechanical properties.

The combined effect of these elements defines 42CrMo4 as a low-alloy structural steel with excellent mechanical properties, particularly suitable for applications involving dynamic loading and for use after heat treatment (quenching and tempering).

Table 1 Chemical composition of steel 42CrMo4

Element	Content, %	Element	Content, %
C	0.38 – 0.45	Si	< 0.40
Cr	0.90 – 1.20	P	< 0.025
Mo	0.15 – 0.30	S	< 0.035
Mn	0.60 – 0.90	Fe	Balance

Table 2 Basic optical and thermophysical parametrers of the material

Parametert	Value
Thermal conductivity k, W/m·K	42.5
Density ρ, kg/m³	7815
Specific heat c, J/(kg·K)	470
Thermal diffusivity a, m²/s	1.157×10^{-5}
Melting temperature T_m, K	1716
Latent heat of melting L_m, J/kg	2.514×10^{5}
Initial temperature T_0, K	293

B. Laser system

The laser hardening experiments were performed using a high-power diode laser system with a maximum output power of 4 kW. The laser operates in continuous wave (CW) mode, providing a stable and uninterrupted energy input, which is essential for uniform surface heating during the hardening process. The emitted radiation lies in the near-infrared spectral range, with a wavelength between 900 and 1080 nm, a range that is well absorbed by ferrous alloys (including steel) and therefore suitable for surface heat treatment applications.

The diode laser system is characterized by a relatively high electrical-to-optical efficiency of approximately 45%, which is significantly higher than that of many other industrial laser types. This high efficiency reduces overall energy consumption and minimizes thermal losses. The beam quality factor ($M^2 = 4$) is typical for high-power diode lasers, indicating a moderately divergent beam that is well suited for applications requiring larger, homogeneous irradiation areas rather than fine focusing.

The laser processing cell was fully automated and consisted of a robotic manipulation system based on a Fanuc M20-iD industrial robot, which ensured precise and repeatable movement of the laser head relative to the workpiece. In addition, a single-axis positioner was integrated into the system to allow controlled rotation or positioning of the samples, enabling uniform treatment of complex geometries and improving process flexibility.

The laser module was powered by an LDM4000-100 laser power supply, which provided stable power delivery and precise control over the laser output parameters. The laser beam was delivered to the workpiece through an OTZ-5 VR laser processing head equipped with vari-optics. This optical system allowed continuous adjustment of the laser spot size within a range from 5 × 8 mm to 22 × 44 mm. Such flexibility in spot size enabled optimization of the energy density and heating profile depending on the specific processing conditions and material requirements.

For real-time process monitoring and control, the system incorporated an integrated two-color pyrometer (Model LDC01, Mergenthaler). This non-contact temperature measurement device operates by detecting thermal radiation at two different wavelengths, allowing accurate temperature readings that are less sensitive to variations in surface emissivity. The pyrometer was used to continuously monitor and regulate the surface temperature during laser hardening, ensuring consistent thermal cycles and preventing overheating or insufficient hardening.

Overall, the combination of a high-power diode laser, adaptable beam shaping, robotic handling, and closed-loop temperature control enabled precise, efficient, and reproducible laser surface hardening operations.

C. *Theoretical aspect*

Laser hardening is a complex technological process, depending on a number of parameters. They are in complex interdependencies with each other. What temperature is obtained on the surface of the material is largely determined by the power density of the laser radiation, the hardening rate and the optical and thermophysical properties of the material. Therefore, there is a relationship between these parameters. It can be obtained from the heat conduction equation and the heat balance equation with certain approximations. For temperatures below the melting point, the power density is given by the expression

$$q_s = \frac{k(T - T_0)}{2A}\sqrt{\frac{\pi v}{ab}}, \quad T < T_0 \tag{1}$$

where T_0 is initial temperature (ambient temperature).

The critical melting power density is given by the expression

$$q_{scm} = \frac{(1+s)\,k\,(T_m - T_0)}{2A}\sqrt{\frac{\pi v}{ab}}, \quad T = T_m \tag{2}$$

where s is parameter, which is given by the formula

$$s = \frac{L_m}{c\,(T_m - T_0)} \quad . \tag{3}$$

D. *Methodology*

The studies to determine the preliminary working density intervals for the hardening process of 42CrMo4 steel samples using a fiber laser proceed in the following sequence:

- Determination of the power density for different speeds at a temperature of 1123 K by formula (1). The necessary material parameters are taken from table 2. Calculations are made for two laser beam profiles, presented in Fig. 1. They are rectangles with dimensions: for the first profile (Fig. 1a) – a = 15 mm and b = 5 mm and for the second profile (Fig. 1b) – a = 5 mm and b = 15 mm.;
- Determination of the critical power density for different speeds by formulas (2) and (3). The necessary material parameters are taken from table 2. Calculations are made for two laser beam profiles;
- From the obtained results, graphs of the dependence of the critical power density and the power density at a temperature of 1123 K on the speed for both laser beam profiles are drawn;
- • The results of the numerical calculations are analyzed and summarized;
- The method is validated with numerical calculations using experimental results that we have obtained at our research center.

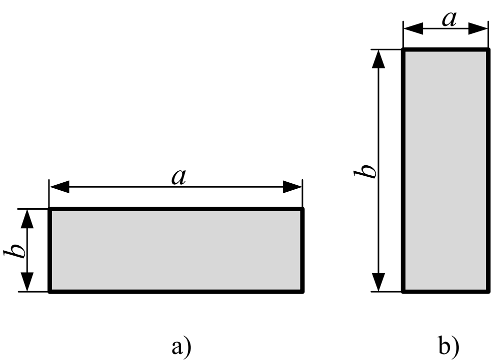

Fig. 1. Laser beam profiles of the fiber laser hardening system

III. RESULTS AND DISCUSSION

According to the adopted methodology, numerical calculations were carried out to determine both the critical power density required for melting and the power density necessary to reach the hardening temperature for different processing speeds. The calculations were based on equations (1) – (3), using the thermophysical parameters of 42CrMo4 steel listed in Table 2. The scanning speed was varied within the range of 3 mm/s to 15 mm/s, with a step of 2 mm/s, in order to cover a representative interval of practical processing conditions.

Two different laser beam profiles were considered in the analysis, corresponding to rectangular spot geometries with dimensions 15 × 5 mm and 5 × 15 mm. These profiles simulate different energy distributions along and across the scanning direction, which significantly affect the thermal field and the resulting hardening conditions.

The calculated results are presented graphically in Figures 2a and 2b, where the dependence of power density on processing speed is illustrated. The blue curves represent the critical power density required to initiate melting of the material, while the green curves correspond to the power density necessary to reach the target hardening temperature (approximately 850 K).

A detailed analysis of these dependencies shows that both the critical power density and the required hardening power density increase nonlinearly with increasing scanning speed. This behavior can be explained by the reduced interaction time between the laser beam and the material at higher speeds. As the exposure time decreases, a higher energy input per unit area (i.e., higher power density) is required to achieve the same thermal effect. This nonlinear trend reflects the transient nature of heat conduction and the increasing dominance of heat dissipation at higher speeds.

An important observation from the graphs is that the feasible operating region for laser hardening is bounded between the two curves. The lower boundary (green curve) represents the minimum power density required to reach the austenitization temperature necessary for phase transformation, while the upper boundary (blue curve) indicates the onset of melting. Therefore, effective laser hardening without surface melting can only be achieved within this process window. This region defines the optimal combination of power density and scanning speed for the given material and beam geometry.

For the first laser beam profile (15 × 5 mm), the critical melting power density varies from approximately 1.33×10^7 W/m² to 2.97×10^7 W/m², while the power density required to reach the hardening temperature ranges from 0.38×10^7 W/m² to 0.84×10^7 W/m² over the investigated speed interval. In contrast, for the second profile (5 × 15 mm), the corresponding values are significantly lower, ranging from 0.77×10^7 W/m² to 1.74×10^7 W/m² for melting, and from 0.22×10^7 W/m² to 0.49×10^7 W/m² for hardening.

The observed difference between the two profiles is primarily due to the variation in energy distribution and heat flow conditions. The elongated profile in the scanning direction (15 × 5 mm) results in a shorter interaction width and higher heat concentration, requiring greater power density to achieve the same thermal penetration. Conversely, the wider profile perpendicular to the scanning direction (5 × 15 mm) promotes more efficient heat accumulation and distribution, thereby reducing the required power density.

Furthermore, the significantly higher values of the critical power density compared to those required for hardening can be attributed to the additional energy needed not only to raise the material temperature to the melting point but also to supply the latent heat of fusion. This energy contribution is substantial and leads to a clear separation between the two curves, ensuring a relatively wide processing window for safe operation.

Overall, the results demonstrate that both scanning speed and beam geometry play a crucial role in determining the thermal response of the material. The selection of appropriate process parameters must therefore consider these factors to ensure sufficient heating for phase transformation while avoiding surface melting. The presented numerical analysis provides a reliable basis for defining such operating intervals, which can subsequently be validated through experimental investigation.

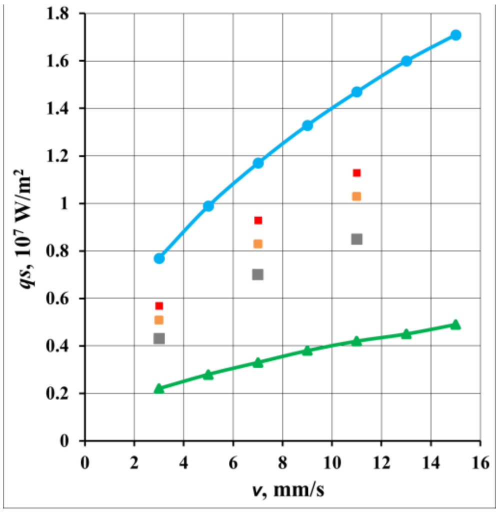

a)

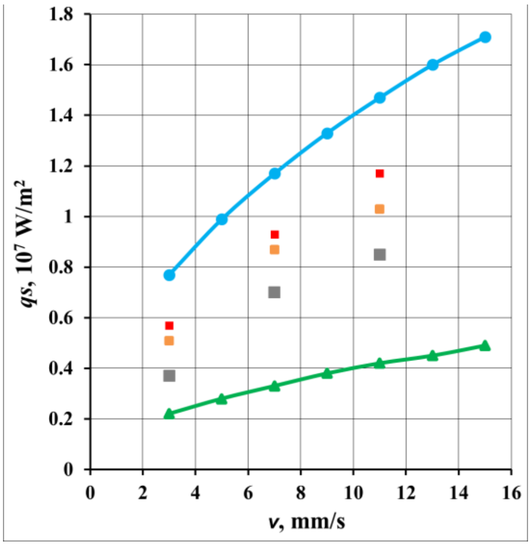

b)

Fig. 2. Graph of the dependence of the critical power density of melting on the speed for steel 42CrMo4 (blue color). Graph of the dependence of the power density on the speed at a temperature of 850 K for steel 42CrMo4 (green color); with laser profiles: a) a = 15 mm and b = 5 mm; b) a = 5 mm and b = 15 mm.

A more detailed analysis of the obtained numerical results shows that the relationship between scanning speed and required power density is strongly nonlinear for both investigated laser beam profiles. This behavior is primarily due to the transient heat transfer conditions during laser-material interaction. As the scanning speed increases, the interaction time between the laser beam and the material surface decreases significantly. Consequently, less time is available for heat to penetrate into the material, and a higher power density is required to achieve the same thermal effect, i.e., to reach the austenitization temperature necessary for hardening.

At lower scanning speeds (3–5 mm/s), the interaction time is relatively long, allowing sufficient heat accumulation even at lower power densities. In this regime, the process is more stable and less sensitive to small variations in parameters. However, as the speed increases beyond 9–11 mm/s, the process becomes increasingly sensitive, and a relatively small increase in speed requires a disproportionately higher increase in power density. This explains the observed nonlinear growth of both the critical melting power density and the hardening power density.

The graphical representation clearly shows that the feasible operating region for laser hardening is confined between the two characteristic curves. The lower boundary corresponds to the minimum energy input required to achieve phase transformation (austenitization), while the upper boundary represents the threshold beyond which surface melting begins. This intermediate region defines the technological window in which effective laser hardening can be performed without undesirable effects such as surface melting, excessive roughness, or microstructural degradation.

A comparison between the two beam profiles reveals a significant influence of the beam geometry on the process parameters. For the first profile (15 × 5 mm), the required power density is consistently higher across the entire speed range. This can be attributed to the elongated geometry in the scanning direction, which reduces the effective interaction time per unit area and leads to increased heat dissipation along the scanning path. As a result, higher energy input is necessary to compensate for these losses.

In contrast, the second profile (5 × 15 mm), which is wider perpendicular to the scanning direction, promotes more efficient heat accumulation in the treated zone. The increased width allows better overlap of thermal fields and reduces heat losses, resulting in lower required power densities. Quantitatively, the required power density for the first profile is approximately 1.7 times higher than that for the second profile under identical processing conditions, confirming the strong dependence of the process on beam shaping.

The analysis of the preliminary operating intervals (Tables 3 and 4) further confirms these observations. It is evident that increasing the scanning speed by a factor of five (from 3 mm/s to 15 mm/s) leads to an increase in the required power density by approximately 2.25 times. This result highlights the importance of careful parameter selection, particularly when aiming to increase productivity through higher processing speeds.

TABLE 3 PRELIMINARY WORKING INTERWALS OF POWER DENSITI I LASER HARDENING OF 42CRMO4 STEEL SAMPLES WITH A DIODE LASER FOR THE FIRST LASER BEAM PROFILE

Speed *v*, mm/s	**Power density q_s, 10^7 W/m²**
3	0.38 – 1.33
5	0.49 – 1.71
7	0.58 – 2.03
9	0.65 – 2.30

11	0.72 – 2.54
13	0.79 – 2.76
15	0.84 – 2.97

TABLE 4 PRELIMINARY WORKING INTERWALS OF POWER DENSITI I LASER HARDENING OF 42CRMO4 STEEL SAMPLES WITH A DIODE LASER FOR THE SECOND LASER BEAM PROFILE

Speed *v*, mm/s	Power density q_s, 10^7 W/m^2
3	0.22 – 0.77
5	0.28 – 0.99
7	0.33 – 1.17
9	0.38 – 1.33
11	0.42 – 1.47
13	0.45 – 1.60
15	0.49 – 1.71

A key aspect of the present study is the comparison between numerical predictions and experimental results. The experimental data points, corresponding to surface temperatures of 1173 K (in gray), 1273 K (in orange), and 1373 K (in red), are located entirely within the region bounded by the calculated curves. This confirms that the numerical model successfully predicts the practical operating window for laser hardening.

Furthermore, the experimental results follow the same trend as the numerical calculations, namely an increase in required power density with increasing scanning speed and target temperature. The slight deviations between numerical and experimental values can be attributed to factors not fully accounted for in the model, such as temperature-dependent material properties, surface oxidation, variations in absorptivity, and heat losses due to convection and radiation.

Despite these simplifications, the observed agreement between numerical and experimental results can be considered very good. This validates the applicability of the proposed numerical approach for preliminary process design and optimization. It demonstrates that relatively simple analytical models, when properly formulated, can provide reliable estimates of the process parameters and significantly reduce the need for extensive experimental trials.

IV. CONCLUSIONS

The present study provides a comprehensive comparative analysis of numerical and experimental results in the laser hardening of 42CrMo4 steel using a high-power diode laser system. Based on the obtained results, the following conclusions can be drawn:

- A numerical approach based on the heat conduction equation and thermal balance principles was successfully applied to determine preliminary operating intervals of laser power density for different scanning speeds.
- The analysis revealed a nonlinear relationship between scanning speed and required power density. Increasing the speed leads to a significant increase in power density due to reduced interaction time and enhanced heat dissipation.
- The feasible process window for laser hardening is clearly defined between the minimum power density required for austenitization and the critical power density for surface melting. This region represents the optimal operating range for achieving high-quality hardening without thermal damage.
- The geometry of the laser beam profile has a substantial influence on the process. The elongated profile in the scanning direction requires approximately 1.7 times higher power density compared to the transverse profile, due to differences in heat distribution and interaction conditions.
- Experimental results obtained at different surface temperatures and scanning speeds show very good agreement with the numerical predictions. All experimental data points fall within the calculated operating intervals, confirming the validity of the proposed model.
- The slight discrepancies between numerical and experimental results are mainly due to simplifying assumptions in the model, such as constant material properties and neglect of certain heat loss mechanisms.
- The developed methodology can be effectively used for preliminary selection of process parameters, reducing the need for extensive experimental trials and improving the efficiency of process design.

From an application point of view, the obtained results have significant practical importance for industrial laser processing:

- The defined operating intervals of power density and scanning speed can be directly used for process optimization in industrial laser hardening systems, reducing the need for costly and time-consuming trial-and-error experiments.
- The results enable predictive selection of process parameters depending on the desired hardening depth and surface quality, which is particularly important in industries such as automotive, aerospace, and heavy machinery, where

components operate under high wear and fatigue conditions.

- The demonstrated influence of beam geometry provides guidance for selection and design of laser optics and beam shaping systems, allowing engineers to tailor the energy distribution according to specific technological requirements.
- The validated numerical model can be integrated into computer-aided manufacturing (CAM) and simulation software, supporting digital process planning and enabling faster implementation of laser hardening technologies in production environments.
- The ability to accurately define the process window contributes to improving process stability, repeatability, and energy efficiency, which are critical factors in modern sustainable manufacturing.
- Furthermore, the methodology can be extended to other steels and laser processing techniques, making it a useful tool for broader applications in laser surface engineering, including hardening, cladding, and surface modification.

In conclusion, the combination of numerical modeling and experimental validation provides a reliable, efficient, and practically applicable approach for optimizing laser hardening processes. The results obtained in this study offer valuable guidance for both industrial practitioners and researchers, contributing to the advancement of laser surface treatment technologies and their wider implementation in engineering practice.

V. Acknowledgment

The authors express their gratitude for the helpful advice and suggestions to all reviewers and organizers to improve the presentation of the performed research. This research was funded by the European Regional Development Fund under the Operational Program "Scientific Research, Innovation and Digitization for Smart Transformation 2021-2027", Project CoC "Smart Mechatronics, Eco- and Energy Saving Systems and Technologies", BG16RFPR002-1.014-0005.

References

[1] W. Steen, J. Mazumder, Laser Material Processing, Fourth Edition, Springer London, ps. 558, 2010, https://doi.org/10.1007/978-1-84996-062-5

[2] J. Ion, Laser Processing of Engineering Materials, Elsevier, ps. 556, 2005, ISBN 978-0-7506-6079-

[3] Ł. Łach, Recent Advances in Laser Surface Hardening: Techniques, Modeling Approaches, and Industrial Applications, Crystals, 14(8):726, 2024, DOI: https://doi.org/10.3390/cryst14080726 [Accessed 13 August 2024]

[4] T. Quan, Overview Study on Laser Surface Hardening Technology and Its Applications, International Journal of Engineering Inventions, Volume 14, Issue 5, pp. 68-75, 2025, ISSN: 2278-7461 [Accessed May 2025]

[5] N. Dahotre and S. Harimkar, Laser Fabrication and Machining of Materials, Springer New York, ps. 558, 2008, https://doi.org/10.1007/978-0-387-72344-0 [Accessed 25 January 2008]

[6] M. Miralles, Laser Hardening of Cutting Tools, Master's Thesis, Lulea University of Technology, 2003, ps. 87, https://www.diva-portal.org/smash/get/diva2:1022680/FULLTEXT01.pdf

[7] W. Deng, X. Gong, C. Du and J. Zhang, Effect of laser hardening on surface properties of high-speed steel, Journal of Physics: Conference Series, Volume 2951 012146, 2024, DOI: https://doi.org/10.1088/1742-6596/2951/1/012146

[8] H. Nguyen, Laser Nd:YAG Surface Hardening to Improve the Durability of Steel Components, Engineering, Technology & Applied Science Research (ETASR), Volume: 15, Issue: 6, pp. 29625-29631, 2025, https://doi.org/10.48084/etasr.14455 [Accepted 27 September 2025]

[9] T. Karadzhov, D. Dichev, I. Zhelezarov, B. Georgiev, D. Pulov and K. Drumev, Improving the accuracy of temperature measurement with thermoresistive sensors, in 2025 XXXV International Scientific Symposium Metrology and Metrology Assurance (MMA), pp. 1–5, 2025, DOI: https://doi.org/10.1109/MMA67107.2025.11311316 [Accepted September 2025]

[10] F. Cordovilla, J. Domínguez, P. Sancho, Á. García-Beltrán and J. Ocaña, Characterization of the surface oxidation reaction and its influence on the radiation absorption during the surface laser hardening process of the 42CrMo4 steel, Revista de Metalurgia, Vol. 52 No. 2, 2016, DOI: https://doi.org/10.3989/revmetalm.2016.v52.i2

[11] I. Černý and J. Sís Fatigue Strength of Laser Hardened 42CrMo4 Steel Considering Effects of Compressive Residual Stresses on Short Crack Growth, Procedia Engineering, 74: 417-420, 2014, DOI: https://doi.org/10.1016/j.proeng.2014.06.292

[12] I. Černý, I. Fürbacher, D. Mikulová and J. Sís, An Effect of Laser Hardening on Contact and Bending Fatigue of a 42CrMo4 Steel, Engineering Materials, 665:221-224, 2015, DOI: https://doi.org/10.4028/www.scientific.net/KEM.665.221 [Accepted September 2015]

[13] C. Soriano, G. Alberdi, J. Lambarri, A. Aranzabe and A. Yáñez, Study of the influence of the oscillation frequency on the surface hardening process of the 42CrMo4 alloy using an oscillating laser beam, Surface and Coatings Technology, Volume 409, 12687715, 2021, https://doi.org/10.1016/j.surfcoat.2021.126877 [Accepted 5 March 2021]

[14] M. Furlani, S. Carvalho and M. Fernandes de Lima, Effect of laser surface hardening on a low carbon steel substrate wear and hardness, 2021, DOI: https://doi.org/10.48550/arXiv.2111.13183 [Accepted November 2021]

[15] S. Reich, D. Heunoske et al. Laser hardening of steel with a 120 kW laser at high throughput, 13th CIRP Conference on Photonic Technologies [LANE 2024], 15-19 September 2024, Fürth, Germany, Procedia CIRP, 124 pp.751–754, 2024, https://doi.org/10.1016/j.procir.2024.08.217 [Accepted January 2024]

[16] N. Dolchinkov, T. Petrov, G. Petrov, C. Tolev and E. Dimitrov, Features of Color Laser Marking on Metals, Environment. Technology. Resources. Proceedings of the 14th International Scientific and Practical Conference, Volume 3, 297-305, https://doi.org/10.17770/etr2023vol3.7222

[17] N. Dolchinkov, Marking and Cutting of Non-metallic Products with CO2 Laser, IOP Publishing Ltd, Journal of Physics: Conference Series, Volume 2224, 2021 2nd International Symposium on Automation, Information and Computing (ISAIC 2021) 03/12/2021 - 06/12/2021, 1742-6588, pp 1-8, 2021, Online ISSN: 1742-6596

[18] H. Zhang, M. Zhu, S. Ji, J. Zhang and H. Fan, Numerical simulation and experimental study on laser hardening process of 42CrMo4 steel, Advances in Mechanical Engineering, 13(9): 168781402110446, 2021, DOI: https://doi.org/10.1177/16878140211044649 [Accepted September 2021]

[19] S. Idelsohn, M. Storti and L. Crivelli, Numerical methods in phase-change problems, Archives of Computational Methods in Engineering, 1(1):49-74, 1994, DOI: https://doi.org/10.1007/BF02736180 [Accepted March 1994]

[20] A. El-Batahgy, R. Ahmed and A-R. Moussa, Laser Surface Hardening of Tool Steels – Experimental and Numerical Analysis, Journal of Surface Engineered Materials and Advanced Technology, 03(02):146-153, 2013, DOI: https://doi.org/10.4236/jsemat.2013.32019 [Accepted January 2013]

[21] Dolchinkov N, Lazov L, Shterev Y., Lilianova St., Pacejs Anton, Use of CO2 laser for marking and clearing of textile materials for manufacture of military equipment , 12th International Scienfic and Practical conference Environment. Technology. Resources. ISBN 1691-5402, Vol 3, 20-22.06.2019 г. Rezekne, Latvia, pp.. 32-36

[22] Korolev I.., Kravchenko, M., Fedorova, E., Dolchinkov, N., Protection of biological objects from electromagnetic radiation, E3S Web of Conferences, 2023, 411, 02003, VI International Conference on Actual Problems of the Energy Complex and Environmental Protection (APEC-VI-2023), https://doi.org/10.1051/e3sconf/202341102003